

Transport Simulation of Transport Barriers and Current Hole in Tokamaks

M. Honda and A. Fukuyama

Department of Nuclear Engineering, Kyoto University, Kyoto, 606-8501, Japan

Transport barriers which contribute to keep high pressure in the core region play a very important role in sustaining a high performance plasma. The understanding of its physical mechanism is one of the most urgent issues in fusion research. In order to achieve a long-pulse high performance discharge, we need to establish the way to control the transport barriers and increase the ratio of the bootstrap current to the total current. In this paper, we examine the validity of the neoclassical transport model of the bootstrap current and compare the results of transport simulation using turbulent transport models with the experimental observations. We also study characteristics of the internal transport barrier (ITB) with a zero current region by carrying out thermal transport simulation.

The 1D transport code TASK/TR solves a set of diffusive transport equations for particle and heat fluxes of thermal species (electron, deuterium, tritium and helium) and poloidal magnetic field, as well as two fast particle components, beam ion and α particle. In addition we mainly use the NCLASS[1] model as a standard neoclassical transport model. We mainly use a ballooning type turbulent transport model, the current diffusive ballooning mode (CDBM) model[2], which successfully reproduced internal transport barrier in the high β_p mode and the reversed shear (RS) mode[2]. We also use two turbulent models based on the ion temperature gradient (ITG) mode; the IFS/PPPL model[3] and GLF23 model[4].

In order to validate turbulent transport models, we have carried out both steady state and time evolution simulations of electron and ion temperatures and compared with experimental profiles from the ITPA profile database[5]. In a steady state simulation we fixed a set of profile data, e.g. density n , safety factor q and NBI heating profiles provided from the database and solve the evolution of T_e and T_i until a stationary state is established, typically within 0.5 s. The set of equations for temperature is solved in the region where a normalized minor radius $\rho < 0.9$, since a definitive H-mode model has not been established yet.

In Fig.1, we show the electron and ion temperature profiles calculated for a DIII-D L-mode discharge using CDBM, IFS/PPPL and GLF23. It is found that for both electron and ion temperatures CDBM reproduced the experimentally observed temperature in the central region. For $\rho > 0.2$ all the models approximately reproduced the experimental T_e profile while the deviation of the T_i profiles from experimental data is relatively large. We found that the two ITG type models produce quite similar T_e profiles.

Because of the recent progress on advanced scenarios, correct evaluation of the bootstrap current in a steady-state operation has become important. Several neoclassical transport models have ever been proposed in terms of the neoclassical plasma resistivity and the bootstrap

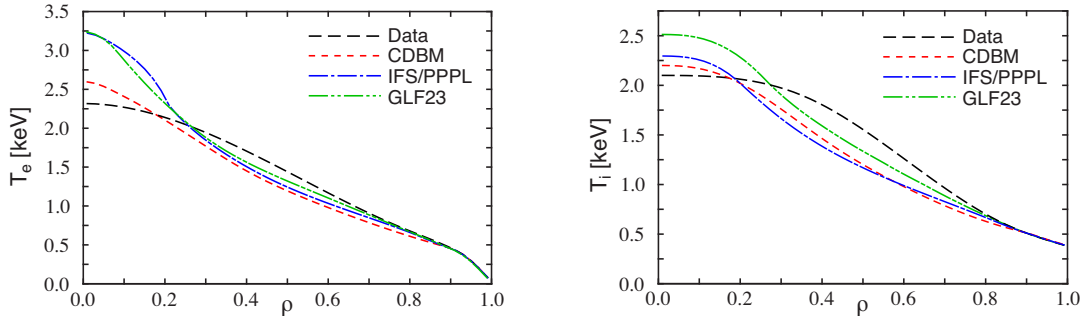


Figure 1: Predicted electron and ion temperatures in the steady state for the experimental data of DIII-D #82188 at $t = 3.775$ s.

current. We have chosen four models for each of the two quantities and compared predicted profiles among four models: Hinton and Hazeltine[6], Hirshman, Hawryluk and Birge[7], Sauter et al.[8] and NCLASS[1] for resistivity, and Hinton and Hazeltine, Hirshman[9], Sauter et al. and NCLASS for bootstrap current.

The result of the simulation is shown in Fig.2, where both the bootstrap current and the resistivity are compared with each other for three different operation modes, i.e. L-mode, high β_p mode and RS configuration. For both the neoclassical resistivity and the bootstrap current, the profiles obtained by using the four models roughly agree with each other. In the L-mode and the high β_p mode, the reason that the bootstrap current profile of Hirshman model exceeds

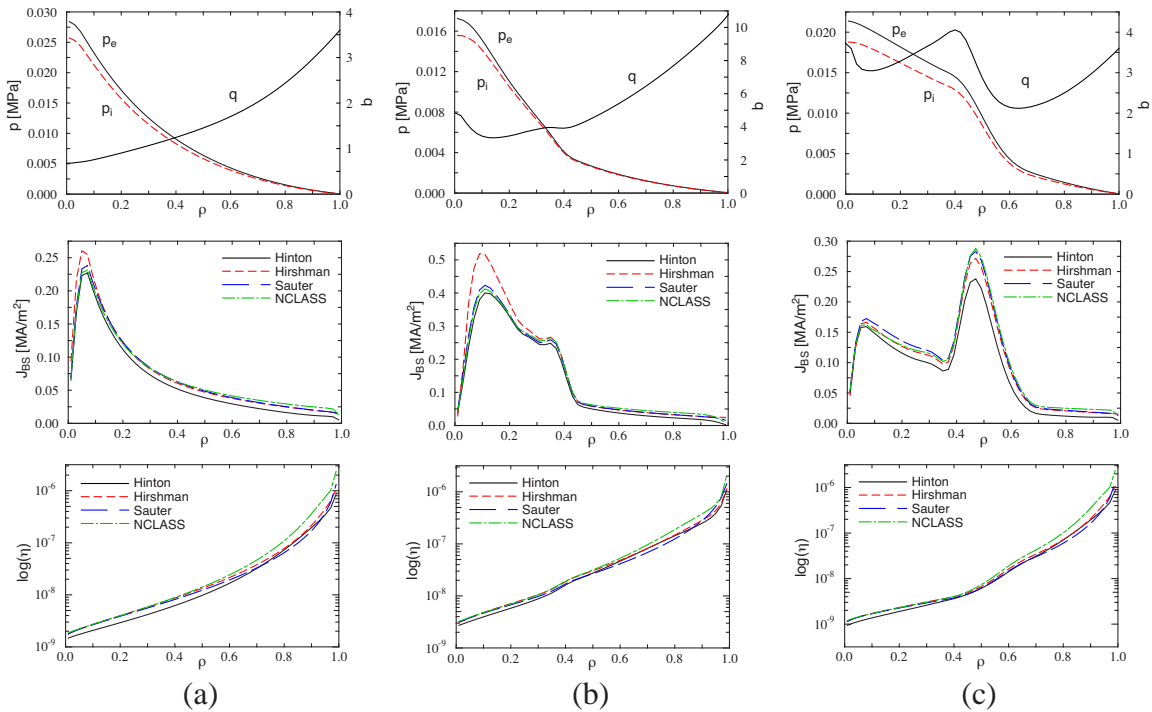


Figure 2: Comparison of the bootstrap current density, J_{BS} , and the resistivity, η , for various neoclassical models. Operation modes are (a) L-mode, (b) high β_p mode and (c) RS configuration. ($R = 3$ m, $a = 1.2$ m, $\kappa = 1.5$, $B_0 = 3$ T)

those of other three models may be attributed to the difference of the trapped particle fraction formula. If the potato orbit effect is included in NCLASS, a neoclassical diffusivity near the magnetic axis slightly changes, but the bootstrap current and the resistivity are hardly affected.

RS configuration with strong ITBs such as the box-type[10] has been considered as a promising candidate of advanced operation scenario. Recently it was observed, owing to the improvements on MSE measurement system, that a region where the current density almost vanishes, a current hole, was stably formed in the central region of JT-60U high performance RS plasmas[11]. The current hole, however, contains phenomena which are not well understood, such as a difficulty in electron current drive. Under these circumstances thermal transport simulation can be a strong tool to clarify the physical mechanism of the current hole formation.

We solve only the thermal transport equations for simplicity. We set the initial temperature as 0.5 keV at the center and 0.25 keV at the edge. As a preconditioning, plasma current was ramped up from 0.1 MA to 0.5 MA during 1 second. Then heating of 6.5 MW at $r_h = 0.25$ m ($\rho \approx 0.21$) was started and the plasma current was ramped up from 0.5 MA to 1 MA during 2 seconds. The simulation results are shown in Fig.3.

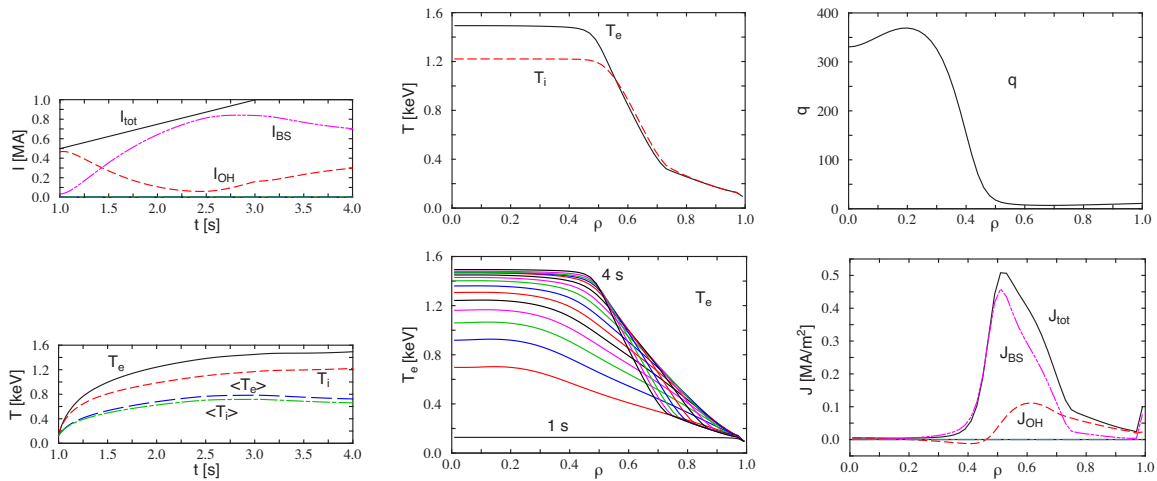


Figure 3: The results of the current hole simulation at $t = 4$ s. Device parameters are the same as those in Figure 2.

We find that in a central region ($\rho < 0.4$) current density is nearly zero whereby the safety factor becomes large and in the outer region ($\rho > 0.4$) quite a large bootstrap current fraction are sustained. ITB shoulders are formed near the minimum q radius and flat temperature profiles are produced inside of it.

The formation of the current hole is sensitive to the edge temperature so that we examined the dependence of the radius of the ITB shoulder (ρ_{shoulder}) and the ITB foot (ρ_{foot}) and electron and ion temperatures at the center (T_e , T_i) on the edge temperatures. The result shown in Fig.4 tells us that with the increase of the edge temperatures, both ρ_{shoulder} and ρ_{foot} increase and the

core region inside the ITB broadens, while both the electron and ion temperatures at the center decrease. Raising the edge temperature makes the resistivity in the edge region decrease and the penetration of the current becomes slow. Since the current density localizes in the outer region, the minimum q and the ITB stays outward.

In Fig.5, the dependence of the input power, P_{in} , for $r_h = 0.25$ m is shown. The current density at the center, J_0 , decreases exponentially, but never becomes negative, with the increase of P_{in} . In the case of $r_h = 0.25$ m the optimum input power which maximizes $T_e(0)$ exists. Further analyses show us that for $r_h < 0.25$ m $T_e(0)$ monotonically increases with the increase of P_{in} and monotonically decreases for $r_h > 0.25$ m. The ITB radii $\rho_{shoulder}$ and ρ_{foot} increase with the increase of P_{in} and the expansion of the volume inside the ITB contributes to the decrease of $T_{e,i}(0)$. The stored energy monotonically increases with increasing P_{in} .

There are still some problems that we have to settle; improvement of the neoclassical transport models in the low B_θ region, coupling with the equilibrium code, and the time evolution of the density. More comprehensive analysis will be reported near future.

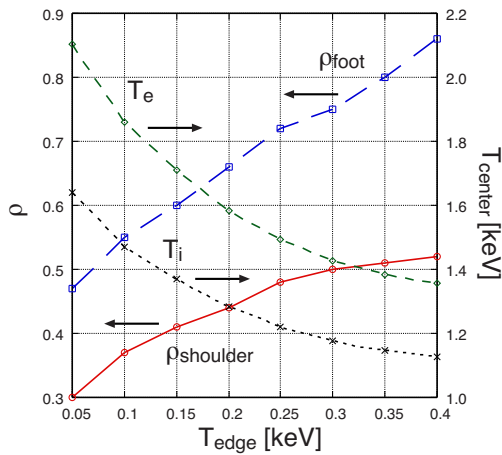


Figure 4: Edge temperature dependency ($P_{input} = 6.5$ MW, $r_h = 0.25$ m).

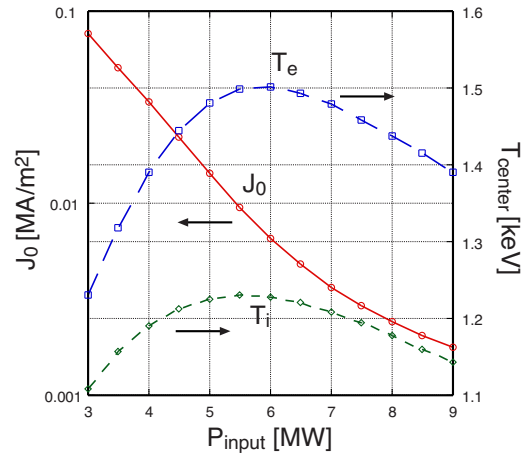


Figure 5: Input power dependency ($T_{edge} = 0.25$ keV, $r_h = 0.25$ m).

- [1] W. A. Houlberg et al.: Phys. Plasmas **4** (1997) 3230.
- [2] A. Fukuyama et al.: Plasma Phys. Control. Fusion **37** (1995) 611.
- [3] M. Kotschenreuther, et al.: Phys. Plasmas **2** (1995) 2381.
- [4] R. E. Waltz et al.: Phys. Plasmas **4** (1997) 2482.
- [5] The ITER 1D Modelling Working Group: Nucl. Fusion **40** (2000) 1955.
- [6] F. L. Hinton et al.: Rev. Mod. Phys. **48** (1976) 239.
- [7] S. P. Hirshman et al.: Nucl. Fusion **17** (1977) 611.
- [8] O. Sauter et al.: Phys. Plasmas **6** (1999) 2834.
- [9] S. P. Hirshman: Phys. Fluids **31** (1988) 3150.
- [10] H. Shirai et al.: Nucl. Fusion **39** (1999) 1713.
- [11] T. Fujita et al.: Phys. Rev. Lett. **87** (2001) 245001.